

Computational Science
Laboratory Report CSL-TR-19-1
December 5, 2019

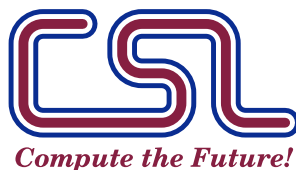
Arash Sarshar, Steven Roberts, and
Adrian Sandu

*“Alternating Directions Implicit
Integration in a General Linear
Method Framework”*

Cite as: Arash Sarshar, Steven Roberts, Adrian Sandu,
Alternating directions implicit integration in a
general linear method framework, Journal of
Computational and Applied Mathematics, 2019, 112619,
<https://doi.org/10.1016/j.cam.2019.112619>.

Computational Science Laboratory
“Compute the Future!”

Department of Computer Science
Virginia Polytechnic Institute and State University
Blacksburg, VA 24060
Phone: (540)-231-2193
Fax: (540)-231-6075
Email: sandu@cs.vt.edu
Web: <http://csl.cs.vt.edu>



Alternating Directions Implicit Integration in a General Linear Method Framework

Arash Sarshar^{a,*}, Steven Roberts^a, Adrian Sandu^a

^a*Computational Science Laboratory
Department of Computer Science
Virginia Tech*

Abstract

Alternating Directions Implicit (ADI) integration is an operator splitting approach to solve parabolic and elliptic partial differential equations in multiple dimensions based on solving sequentially a set of related one-dimensional equations. Classical ADI methods have order at most two, due to the splitting errors. Moreover, when the time discretization of stiff one-dimensional problems is based on Runge-Kutta schemes, additional order reduction may occur. This work proposes a new ADI approach based on the partitioned General Linear Methods framework. This approach allows the construction of high order ADI methods. Due to their high stage order, the proposed methods can alleviate the order reduction phenomenon seen with other schemes. Numerical experiments are shown to provide further insight into the accuracy, stability, and applicability of these new methods.

Keywords: Initial value problems, time integration, IMEX methods, alternating directions AMS 65L05, AMS 65L07

1. Introduction

We are concerned with solving the initial value problem:

$$y'(t) = f(y) = \sum_{\sigma=1}^N f^{\{\sigma\}}(y), \quad y(t_0) = y_0, \quad (1)$$

where the right hand side function $f : \mathbb{R}^d \rightarrow \mathbb{R}^d$ is additively split into N partitions. Systems such as eq. (1) emerge from method of lines semi-discretization of PDEs when all spatial derivatives are approximated by their discretization. In many cases, the right hand side function includes discrete self-adjoint operators

*Corresponding author

Email addresses: sarshar@vt.edu (Arash Sarshar), steven94@vt.edu (Steven Roberts), sandu@cs.vt.edu (Adrian Sandu)

performing spatial derivatives in different directions. The sparsity structure of these operators is similar, for example, in the case when a fixed-stencil finite difference method is used to resolve spatial derivatives. Implicit time-stepping methods are preferred to propagate stiff differential equations in time, but they require working with large Jacobian matrices. Implicit-Explicit (IMEX) methods allow us to integrate non-stiff parts of the system more efficiently, however, more can be achieved by designing specialized time-stepping methods for certain classes of problems. Depending on the choice of discretization, we can use the tensor product structure of derivative operators to only work with one-dimensional Jacobian matrices much smaller than the full Jacobian, applying directional derivatives in different directions in turn.

Alternating Directions Implicit (ADI) schemes for parabolic problems were first introduced in the works of Douglas [1], Douglas and Rachford [2], and Peaceman and Rachford [3]. Closely related to this field is the body of work on operator splitting schemes [4–6] and Approximate Matrix Factorizations (AMF) applied to Rosenbrock-W [7–9] and LIRK methods [10]. Another important development is the Fractional Step Runge–Kutta framework [11, 12] investigating the link between directional methods and IMEX schemes.

Early analysis of convergence of stiff ODEs can be traced back to Prothero–Robinson [13]. Ostermann *et al.* formally show the fractional order phenomenon is related to changes in the behavior of local truncation error in stiff systems [14]. Methods of high stage order are known to alleviate this drawback [15, 16]. The General Linear Method (GLM) framework [17–19] encompasses many of these methods and facilitates creation of new ones for novel applications. The theory of partitioned GLMs was formalized in [20] and different families of methods based on this structure have been reported in [21–24]. More recent high order IMEX-GLMs found in the literature [25–27] are based on Diagonally Implicit Multistage Integration Methods (DIMSIMs), Two-Step Runge–Kutta methods, and Peer methods providing various accuracy and stability enhancements.

The goal of this paper is to extend the capabilities of ADI schemes to high order GLMs, creating methods resilient to order reduction while leveraging the efficiency of alternating implicit integration. The paper is organized as follows: We start by reviewing the partitioned GLM framework in section 2, introduce the structure of ADI-GLMs in section 3, study their order conditions in section 4, and investigate their stability in section 5. We comment on design principles and implementation aspects in section 6 followed by numerical experiments in section 7 and the concluding remarks in section 8. Appendix A includes the coefficients of the new methods, and Appendix B presents stability plots.

2. Traditional and partitioned General Linear Methods

A traditional GLM with s internal and r external stages represented by Butcher tableau:

$$\begin{array}{c|cc} \mathbf{c} & \mathbf{A} & \mathbf{U} \\ \hline & \mathbf{B} & \mathbf{V} \end{array}, \quad (2)$$

advances the numerical solution to eq. (1) with timestep h according to:

$$Y_i = h \sum_{j=1}^s a_{i,j} f(Y_j) + \sum_{j=1}^r u_{i,j} \xi_j^{[n-1]}, \quad i = 1, \dots, s, \quad (3a)$$

$$\xi_i^{[n]} = h \sum_{j=1}^s b_{i,j} f(Y_j) + \sum_{j=1}^r v_{i,j} \xi_j^{[n-1]}, \quad i = 1, \dots, r, \quad (3b)$$

where the matrix notation of coefficients is used:

$$\begin{aligned} \mathbf{A} &:= [a_{i,j}] \in \mathbb{R}^{s \times s}, & \mathbf{U} &:= [u_{i,j}] \in \mathbb{R}^{s \times r}, & \mathbf{B} &:= [b_{i,j}] \in \mathbb{R}^{r \times s}, \\ \mathbf{V} &:= [v_{i,j}] \in \mathbb{R}^{r \times r}, & \mathbf{W} &:= [w_{i,j}] = [\mathbf{w}_0 \dots \mathbf{w}_p] \in \mathbb{R}^{r \times (p+1)}, \end{aligned} \quad (4)$$

where matrix \mathbf{W} determines the relation between external stages and derivatives of the exact solution such that for a method of order p :

$$\xi_i^{[n]} = \sum_{k=0}^p w_{i,k} h^k y^{(k)}(t_n) + \mathcal{O}(h^{p+1}).$$

GLM framework is extensive and well-established. Readers interested in theoretical foundation of these methods are referred to the literature [17–19].

IMEX-GLMs are extensions of traditional GLMs that treat partitions of the right hand side with different methods while keeping a single set of internal and external stages. One step of an IMEX-GLM formally reads as:

$$Y_i = h \sum_{\sigma=1}^N \sum_{j=1}^s a_{i,j}^{\{\sigma\}} f^{\{\sigma\}}(Y_j) + \sum_{j=1}^r u_{i,j} \xi_j^{[n-1]}, \quad i = 1, \dots, s, \quad (5a)$$

$$\xi_i^{[n]} = h \sum_{\sigma=1}^N \sum_{j=1}^s b_{i,j}^{\{\sigma\}} f^{\{\sigma\}}(Y_j) + \sum_{j=1}^r v_{i,j} \xi_j^{[n-1]}, \quad i = 1, \dots, r. \quad (5b)$$

3. Formulation of ADI-GLMs

We rely on the theory of IMEX-GLMs as reported in [20, 22, 23] to design partitioned GLMs suited for ADI integration. The goal is to construct GLMs that apply implicit integration to individual partitions of the right hand side function in eq. (1), while using an explicit coupling to the other components. We seek to achieve high stage order while benefiting from the low computational cost of directional implicit methods.

Definition 1 (ADI-GLM schemes). *One step of an N -way partitioned ADI-*

GLM applied to eq. (1) is defined as:

$$Y_i^{\{\mu\}} = h \sum_{\sigma=1}^N \sum_{j=1}^s a_{i,j}^{\{\mu,\sigma\}} f^{\{\sigma\}}(Y_j^{\{\sigma\}}) + \sum_{\sigma=1}^N \sum_{j=1}^r u_{i,j}^{\{\mu,\sigma\}} \xi_j^{\{\sigma\}[n-1]}, \quad (6a)$$

$$i = 1, \dots, s, \quad \mu = 1, \dots, N,$$

$$\xi_i^{\{\mu\}[n]} = h \sum_{\sigma=1}^N \sum_{j=1}^s b_{i,j}^{\{\mu,\sigma\}} f^{\{\sigma\}}(Y_j^{\{\sigma\}}) + \sum_{\sigma=1}^N \sum_{j=1}^r v_{i,j}^{\{\mu,\sigma\}} \xi_j^{\{\sigma\}[n-1]}, \quad (6b)$$

$$i = 1, \dots, r, \quad \mu = 1, \dots, N.$$

Here, we are interested in applying different combinations of explicit and diagonally implicit methods to the right hand side partitions and storing the resulting internal and external stages separately.

If the method is order p , the external stages are related to derivatives of y by:

$$\xi_i^{\{\mu\}[n]} = w_{i,0}^{\{\mu\}} y(t_n) + \sum_{\sigma=1}^N \sum_{k=1}^p w_{i,k}^{\{\mu,\sigma\}} h^k (f^{\{\sigma\}})^{(k-1)}(y(t_n)) + \mathcal{O}(h^{p+1}), \quad (7)$$

$$\mathbf{W}^{\{\mu,\sigma\}} := [\mathbf{w}_0^{\{\mu\}} \dots \mathbf{w}_p^{\{\mu,\sigma\}}] \in \mathbb{R}^{r \times (p+1)}. \quad (8)$$

The method is stage order q if internal stages are approximations of the exact solution at abscissa points $\mathbf{c}^{\{\mu\}}$:

$$Y_i^{\{\mu\}} = y(t_{n-1} + \mathbf{c}_i^{\{\mu\}} h) + \mathcal{O}(h^{q+1}). \quad (9)$$

4. Construction of ADI-GLMs

We start by considering a pair of explicit and implicit GLMs with the same number of external and internal stages:

$$\frac{\mathbf{c}^{\{E\}} \mid \mathbf{A}^{\{E\}} \mid \mathbf{U}^{\{E\}}}{\mathbf{B}^{\{E\}} \mid \mathbf{V}^{\{E\}}}, \quad \frac{\mathbf{c}^{\{I\}} \mid \mathbf{A}^{\{I\}} \mid \mathbf{U}^{\{I\}}}{\mathbf{B}^{\{I\}} \mid \mathbf{V}^{\{I\}}}. \quad (10)$$

We construct ADI-GLMs using a collection of IMEX-GLMs each performing implicit integration in a specific direction. A preconsistent IMEX-GLM has order p and stage order $q \in \{p, p-1\}$ if and only if the following conditions

hold:

$$\frac{\mathbf{c}^{\{\sigma\} \times k}}{k!} - \frac{\mathbf{A}\mathbf{c}^{\{\sigma\} \times (k-1)}}{(k-1)!} - \mathbf{U}^{\{\sigma\}} \mathbf{w}_k^{\{\sigma\}} = 0, \quad (11a)$$

$$k = \{1, \dots, q\}, \quad \sigma \in \{E, I\},$$

$$\sum_{l=0}^k \frac{\mathbf{w}_{k-l}^{\{\sigma\}}}{l!} - \frac{\mathbf{B}^{\{\sigma\}} \mathbf{c}^{\{\sigma\} \times (k-1)}}{(k-1)!} - \mathbf{V}^{\{\sigma\}} \mathbf{w}_k^{\{\sigma\}} = 0, \quad (11b)$$

$$k = \{1, \dots, p\}, \quad \sigma \in \{E, I\}.$$

The structure of the Butcher tableau for an ADI-GLM depends on the number of partitions and number of stiff partitions that require implicit treatment. Here, we focus on three practical examples and more elaborate designs follow the same principles. The Butcher tableau for a 3-way partitioned ADI-GLM with alternating implicit stages in all partitions is:

$$\begin{array}{c|ccc|ccc} \mathbf{c} & \mathbf{A}^{\{I\}} & \mathbf{A}^{\{E\}} & \mathbf{A}^{\{E\}} & \mathbf{U} & \mathbf{0} & \mathbf{0} \\ \mathbf{c} & \mathbf{A}^{\{I\}} & \mathbf{A}^{\{I\}} & \mathbf{A}^{\{E\}} & \mathbf{0} & \mathbf{U} & \mathbf{0} \\ \mathbf{c} & \mathbf{A}^{\{I\}} & \mathbf{A}^{\{I\}} & \mathbf{A}^{\{I\}} & \mathbf{0} & \mathbf{0} & \mathbf{U} \\ \hline & \mathbf{B}^{\{I\}} & \mathbf{B}^{\{E\}} & \mathbf{B}^{\{E\}} & \mathbf{V} & \mathbf{0} & \mathbf{0} \\ & \mathbf{B}^{\{I\}} & \mathbf{B}^{\{I\}} & \mathbf{B}^{\{E\}} & \mathbf{0} & \mathbf{V} & \mathbf{0} \\ & \mathbf{B}^{\{I\}} & \mathbf{B}^{\{I\}} & \mathbf{B}^{\{I\}} & \mathbf{0} & \mathbf{0} & \mathbf{V} \end{array}. \quad (12)$$

When only two partitions are stiff, the non-stiff partition is carried through explicitly:

$$\begin{array}{c|ccc|ccc} \mathbf{c} & \mathbf{A}^{\{I\}} & \mathbf{A}^{\{E\}} & \mathbf{A}^{\{E\}} & \mathbf{U} & \mathbf{0} & \mathbf{0} \\ \mathbf{c} & \mathbf{A}^{\{I\}} & \mathbf{A}^{\{I\}} & \mathbf{A}^{\{E\}} & \mathbf{0} & \mathbf{U} & \mathbf{0} \\ \mathbf{c} & \mathbf{A}^{\{I\}} & \mathbf{A}^{\{I\}} & \mathbf{A}^{\{E\}} & \mathbf{0} & \mathbf{0} & \mathbf{U} \\ \hline & \mathbf{B}^{\{I\}} & \mathbf{B}^{\{E\}} & \mathbf{B}^{\{E\}} & \mathbf{V} & \mathbf{0} & \mathbf{0} \\ & \mathbf{B}^{\{I\}} & \mathbf{B}^{\{I\}} & \mathbf{B}^{\{E\}} & \mathbf{0} & \mathbf{V} & \mathbf{0} \\ & \mathbf{B}^{\{I\}} & \mathbf{B}^{\{I\}} & \mathbf{B}^{\{E\}} & \mathbf{0} & \mathbf{0} & \mathbf{V} \end{array}. \quad (13)$$

We notice immediately that $Y_i^{\{3\}} \equiv Y_i^{\{2\}}$, therefore one only computes two types of stage vectors, and the second is used as an argument for the explicit integration of the third, non-stiff component.

In a similar fashion, a 2-way partitioned ADI-GLM is described by:

$$\begin{array}{c|cc|cc} \mathbf{c} & \mathbf{A}^{\{I\}} & \mathbf{A}^{\{E\}} & \mathbf{U} & \mathbf{0} \\ \mathbf{c} & \mathbf{A}^{\{I\}} & \mathbf{A}^{\{I\}} & \mathbf{0} & \mathbf{U} \\ \hline & \mathbf{B}^{\{I\}} & \mathbf{B}^{\{E\}} & \mathbf{V} & \mathbf{0} \\ & \mathbf{B}^{\{I\}} & \mathbf{B}^{\{I\}} & \mathbf{0} & \mathbf{V} \end{array}. \quad (14)$$

Remark 1. Comparing eqs. (12) to (14) with eq. (6), notice that we have chosen:

$$\mathbf{c}^{\{E\}} = \mathbf{c}^{\{I\}} = \mathbf{c}, \quad (15a)$$

$$\mathbf{U}^{\{E\}} = \mathbf{U}^{\{I\}} = \mathbf{U}, \quad (15b)$$

$$\mathbf{V}^{\{E\}} = \mathbf{V}^{\{I\}} = \mathbf{V}. \quad (15c)$$

This selection is practically useful in creating IMEX-GLMs with unified internal stages. In the context of ADI-GLMs this choice allows us to keep the number of internal and external stages as low as the number of stiff partitions.

Remark 2. We have also decoupled computations involving the external stages:

$$\mathbf{U}^{\{\sigma,\mu\}} = \begin{cases} \mathbf{0} & \sigma \neq \mu \\ \mathbf{U} & \sigma = \mu \end{cases}, \quad \mathbf{V}^{\{\sigma,\mu\}} = \begin{cases} \mathbf{0} & \sigma \neq \mu \\ \mathbf{V} & \sigma = \mu \end{cases}. \quad (16)$$

Theorem 1. The ADI-GLMs eq. (6) subject to eqs. (15) and (16) is stage order q and order p , hereafter denoted by order (q, p) , if and only if individual methods (10) are order (q, p) .

Proof. We first assume that the ADI-GLM is order (q, p) such that eqs. (7) and (9) hold. Since all internal stages $Y_i^{\{\sigma\}}$ share the same abscissa, from eq. (9) we have:

$$Y_i^{\{\sigma\}} = Y_i^{\{\mu\}} + \mathcal{O}(h^{q+1}), \quad \sigma, \mu \in \{1, \dots, N\}. \quad (17)$$

Therefore, we can replace $Y_j^{\{\sigma\}}$ with $Y_j^{\{\mu\}}$ in eq. (6a) without changing the order. The resulting method is an IMEX-GLM with

$$\frac{\mathbf{c} \left| \begin{array}{ccc} \mathbf{A}^{\{\mu,1\}} & \dots & \mathbf{A}^{\{\mu,N\}} \end{array} \right| \mathbf{U}}{\left| \begin{array}{ccc} \mathbf{B}^{\{\mu,1\}} & \dots & \mathbf{B}^{\{\mu,N\}} \end{array} \right| \mathbf{V}}, \quad \mu \in \{1, \dots, N\}. \quad (18)$$

From IMEX-GLM order conditions [20, 28] method (18) is order (q, p) if and only if individual methods

$$\frac{\mathbf{c} \left| \begin{array}{c} \mathbf{A}^{\{\mu,\sigma\}} \end{array} \right| \mathbf{U}}{\left| \begin{array}{c} \mathbf{B}^{\{\mu,\sigma\}} \end{array} \right| \mathbf{V}}, \quad \mu \in \{1, \dots, N\}, \quad \sigma \in \{1, \dots, N\}.$$

are order (q, p) . This means that the methods in eq. (10) have to be order (q, p) .

The *if* part of the theorem can be proven along the same line of reasoning. Assuming individual methods (10) are order (q, p) the IMEX-GLM (18) is order (q, p) . Internal stage values in eq. (5a) can be replaced by an approximation of the same order as in eq. (17) to create the internal stages for ADI-GLM. Since the order of internal stages has not changed, external stages also remain order p . This concludes the proof. \square

Remark 3. *A corollary to theorem 1 is that in the case of ADI-GLM (13), we can forgo computing $(Y_i^{\{3\}}, \xi^{\{3\}[n]})$ stages without losing accuracy. Furthermore, this choice will not affect the stability since the stiff partitions are still treated implicitly and the integration of the non-stiff partition already appears in stage computations.*

5. Stability of ADI-GLMs

Applying the ADI-GLM (12) to the linear scalar test equation:

$$u' = \lambda_x u + \lambda_y u + \lambda_z u, \quad (19)$$

and using eq. (6) leads to the following directional stages:

$$Y^{\{1\}} = \eta_x \mathbf{A}^{\{I\}} Y^{\{1\}} + \eta_y \mathbf{A}^{\{E\}} Y^{\{2\}} + \eta_z \mathbf{A}^{\{E\}} Y^{\{3\}} + \mathbf{U} \xi^{\{1\}[n-1]}, \quad (20a)$$

$$Y^{\{2\}} = \eta_x \mathbf{A}^{\{I\}} Y^{\{1\}} + \eta_y \mathbf{A}^{\{I\}} Y^{\{2\}} + \eta_z \mathbf{A}^{\{E\}} Y^{\{3\}} + \mathbf{U} \xi^{\{2\}[n-1]}, \quad (20b)$$

$$Y^{\{3\}} = \eta_x \mathbf{A}^{\{I\}} Y^{\{1\}} + \eta_y \mathbf{A}^{\{I\}} Y^{\{2\}} + \eta_z \mathbf{A}^{\{I\}} Y^{\{3\}} + \mathbf{U} \xi^{\{3\}[n-1]}, \quad (20c)$$

$$\xi^{\{1\}[n]} = \eta_x \mathbf{B}^{\{I\}} Y^{\{1\}} + \eta_y \mathbf{B}^{\{E\}} Y^{\{2\}} + \eta_z \mathbf{B}^{\{E\}} Y^{\{3\}} + \mathbf{V} \xi^{\{1\}[n-1]}, \quad (20d)$$

$$\xi^{\{2\}[n]} = \eta_x \mathbf{B}^{\{I\}} Y^{\{1\}} + \eta_y \mathbf{B}^{\{E\}} Y^{\{2\}} + \eta_z \mathbf{B}^{\{E\}} Y^{\{3\}} + \mathbf{V} \xi^{\{2\}[n-1]}, \quad (20e)$$

$$\xi^{\{3\}[n]} = \eta_x \mathbf{B}^{\{I\}} Y^{\{1\}} + \eta_y \mathbf{B}^{\{I\}} Y^{\{2\}} + \eta_z \mathbf{B}^{\{I\}} Y^{\{3\}} + \mathbf{V} \xi^{\{3\}[n-1]}, \quad (20f)$$

where $\eta_x = h\lambda_x, \eta_y = h\lambda_y, \eta_z = h\lambda_z$. Defining auxiliary notations $\mathbf{Z} = \text{blkdiag}(\eta_x \mathbf{I}_{s \times s}, \eta_y \mathbf{I}_{s \times s}, \eta_z \mathbf{I}_{s \times s})$ and $\xi^{[n]} = (\xi^{\{1\}[n]}, \xi^{\{2\}[n]}, \xi^{\{3\}[n]})^T$, the stability matrix is defined as:

$$\xi^{[n]} = \mathbf{M}(\eta_x, \eta_y, \eta_z) \xi^{[n-1]}, \quad (21a)$$

$$\mathbf{M}(\eta_x, \eta_y, \eta_z) = \tilde{\mathbf{V}} + \tilde{\mathbf{B}} \mathbf{Z} (\mathbf{I}_{3s \times 3s} - \tilde{\mathbf{A}} \mathbf{Z})^{-1} \tilde{\mathbf{U}}, \quad (21b)$$

where:

$$\tilde{\mathbf{A}} = \begin{bmatrix} \mathbf{A}^{\{I\}} & \mathbf{A}^{\{E\}} & \mathbf{A}^{\{E\}} \\ \mathbf{A}^{\{I\}} & \mathbf{A}^{\{I\}} & \mathbf{A}^{\{E\}} \\ \mathbf{A}^{\{I\}} & \mathbf{A}^{\{I\}} & \mathbf{A}^{\{I\}} \end{bmatrix}, \quad \tilde{\mathbf{U}} = \mathbf{I}_{3 \times 3} \otimes \mathbf{U}, \quad (22a)$$

$$\tilde{\mathbf{B}} = \begin{bmatrix} \mathbf{B}^{\{I\}} & \mathbf{B}^{\{E\}} & \mathbf{B}^{\{E\}} \\ \mathbf{B}^{\{I\}} & \mathbf{B}^{\{I\}} & \mathbf{B}^{\{E\}} \\ \mathbf{B}^{\{I\}} & \mathbf{B}^{\{I\}} & \mathbf{B}^{\{I\}} \end{bmatrix}, \quad \tilde{\mathbf{V}} = \mathbf{I}_{3 \times 3} \otimes \mathbf{V}. \quad (22b)$$

When the eigenvalues of the system (19) are equal in all directions such that $\eta_x = \eta_y = \eta_z = \eta$ the stability matrix becomes:

$$\widehat{\mathbf{M}}(\eta) = \mathbf{M}(\eta, \eta, \eta) = \tilde{\mathbf{V}} + \eta \tilde{\mathbf{B}} \left(\mathbf{I}_{3s \times 3s} - \eta \tilde{\mathbf{A}} \right)^{-1} \tilde{\mathbf{U}}. \quad (23)$$

Equation (23) provides practical means for assessment and optimization of stability of ADI-GLMs.

Remark 4. *The stability regions for individual explicit and implicit methods are defined as:*

$$\mathcal{S}^{\{\sigma\}} = \left\{ \eta \in \mathbb{C} : \mathbf{M}^{\{\sigma\}}(\eta) \text{ power bounded} \right\}, \quad (24a)$$

$$\mathbf{M}^{\{\sigma\}}(\eta) = \mathbf{V}^{\{\sigma\}} + \eta \mathbf{B}^{\{\sigma\}} \left(\mathbf{I}_{s \times s} - \eta \mathbf{A}^{\{\sigma\}} \right)^{-1} \mathbf{U}^{\{\sigma\}}, \quad \sigma \in \{E, I\}. \quad (24b)$$

The stability region of a 3-way partition method is defined as:

$$S = \{ \eta_x, \eta_y, \eta_z \in \mathbb{C} : \mathbf{M}(\eta_x, \eta_y, \eta_z) \text{ power bounded} \}. \quad (25)$$

Remark 5. *To investigate the stability of ADI-GLMs we define real and complex stability regions as:*

$$\mathcal{S}_{\text{Real}} = \{ \eta_x, \eta_y \in \mathbb{R} : \mathbf{M}(\eta_x, \eta_y, \max(\eta_x, \eta_y)) \text{ power bounded} \}, \quad (26a)$$

$$\mathcal{S}_{\text{Cplx}} = \left\{ \eta \in \mathbb{C} : \widehat{\mathbf{M}}(\eta) \text{ power bounded} \right\}. \quad (26b)$$

Remark 6 (Stability as all partitions become infinitely stiff). *Consider the stability matrix eq. (23) when the eigenvalues in each direction simultaneously approach $-\infty$:*

$$\lim_{\eta \rightarrow -\infty} \widehat{\mathbf{M}}(\eta) = \begin{bmatrix} \mathbf{V}^{\{I\}} - (\mathbf{B}^{\{I\}} - \mathbf{B}^{\{E\}}) (\mathbf{A}^{\{I\}} - \mathbf{A}^{\{E\}})^{-1} \mathbf{U} & * \\ \mathbf{0} & \mathbf{M}^{\{I\}}(-\infty) \end{bmatrix}. \quad (27)$$

Due to the block triangular structure of this matrix, the eigenvalues of eq. (27) are the eigenvalues of the diagonal blocks and the entries in the upper right block can be ignored.

Consider the case $p = q = r = s$. We will further assume $\mathbf{w}_0^{\{I\}} = \mathbf{w}_0^{\{E\}}$,

which comes at no loss of generality since we can always pick an equivalent formulation of the base methods where this holds. Using the difference of the order conditions of the base methods, we have that

$$\left(\mathbf{A}^{\{I\}} - \mathbf{A}^{\{E\}}\right) \mathbf{C} + \mathbf{U} \left(\mathbf{W}_{:,1:p}^{\{I\}} - \mathbf{W}_{:,1:p}^{\{E\}}\right) = \mathbf{0}, \quad (28a)$$

$$\left(\mathbf{W}_{:,1:p}^{\{I\}} - \mathbf{W}_{:,1:p}^{\{E\}}\right) \boldsymbol{\mu} - \left(\mathbf{B}^{\{I\}} - \mathbf{B}^{\{E\}}\right) \mathbf{C} - \mathbf{V} \left(\mathbf{W}_{:,1:p}^{\{I\}} - \mathbf{W}_{:,1:p}^{\{E\}}\right) = \mathbf{0}, \quad (28b)$$

where

$$\mu_{i,j} = \begin{cases} 0 & i > j \\ \frac{1}{(j-i)!} & i \leq j \end{cases}, \quad \mathbf{C} = \begin{bmatrix} \mathbb{1}_s & \mathbf{c} & \frac{\mathbf{c}^2}{2} & \cdots & \frac{\mathbf{c}^{p-1}}{(p-1)!} \end{bmatrix}. \quad (29)$$

Now we have that

$$\begin{aligned} & \left(\mathbf{V}^{\{I\}} - \left(\mathbf{B}^{\{I\}} - \mathbf{B}^{\{E\}}\right) \left(\mathbf{A}^{\{I\}} - \mathbf{A}^{\{E\}}\right)^{-1} \mathbf{U}\right) \left(\mathbf{W}_{:,1:p}^{\{I\}} - \mathbf{W}_{:,1:p}^{\{E\}}\right) \\ &= \mathbf{V}^{\{I\}} \left(\mathbf{W}_{:,1:p}^{\{I\}} - \mathbf{W}_{:,1:p}^{\{E\}}\right) + \left(\mathbf{B}^{\{I\}} - \mathbf{B}^{\{E\}}\right) \mathbf{C} \\ &= \left(\mathbf{W}_{:,1:p}^{\{I\}} - \mathbf{W}_{:,1:p}^{\{E\}}\right) \boldsymbol{\mu}. \end{aligned} \quad (30)$$

Thus, the upper left block of eq. (27) is similar to $\boldsymbol{\mu}$ provided $\mathbf{W}_{:,1:p}^{\{I\}} - \mathbf{W}_{:,1:p}^{\{E\}}$ is non-singular. In this case, eq. (27) is not power bounded because the 1 eigenvalue of $\boldsymbol{\mu}$ is defective. We note that this is not an issue when only a single eigenvalue becomes infinitely stiff.

In Appendix B we provide plots of different stability regions for ADI-GLMs.

6. Design and implementation of ADI-GLMs

We have chosen the GLMs to be DIMSIMs [29] in order to reduce the number of free parameters in the design and simplify the order conditions. We require:

$$a_{i,i}^{\{I\}} = \gamma, \quad a_{i,i}^{\{E\}} = 0, \quad a_{i,j}^{\{\sigma\}} = 0, \quad \text{for } j > i, \quad \sigma \in \{E, I\}, \quad (31a)$$

$$\mathbf{U}^{\{\sigma\}} = \mathbf{I}_{s \times r}, \quad \sigma \in \{E, I\}, \quad (31b)$$

$$\mathbf{V}^{\{\sigma\}} = \mathbb{1}_r^T v, \quad v^T \mathbb{1}_r = 1, \quad \sigma \in \{E, I\}. \quad (31c)$$

ADI-DIMSIMs derived in this paper have $p = q = r = s$. The design process starts with choosing the abscissa vector \mathbf{c} . The remaining free parameters are coefficients of $\mathbf{A}^{\{E\}}$, $\mathbf{A}^{\{I\}}$, and v . For the new second and third order schemes, we picked existing, L-stable, type 2 DIMSIMs for $\mathbf{A}^{\{I\}}$ and v . Then, we choose $\mathbf{A}^{\{E\}}$ by numerically optimizing the area of the $\mathcal{S}_{\text{Cplx}}$ and $\mathcal{S}^{\{E\}}$ stability regions using Mathematica. At fourth order, we performed the same optimization for $\mathbf{A}^{\{E\}}$, however, we were unable to achieve satisfactory stability when using an

existing type 2 DIMSIM for the implicit base method. Instead, we derived a new $A(83^\circ)$ -stable DIMSIM for which the ADI-GLM stability was acceptable.

Once $\mathbf{A}^{\{E\}}$ and $\mathbf{A}^{\{I\}}$ and v are determined, $\mathbf{B}^{\{E\}}$ and $\mathbf{B}^{\{I\}}$ are given using DIMSIM formulas [30, 31]. $\mathbf{W}^{\{I\}}$ and $\mathbf{W}^{\{E\}}$ are computed by solving eq. (11) and used in the starting procedure to generate initial values of the external stages at the beginning of the time-stepping loop in eq. (6). The starting procedure consists of integrating the system eq. (1) exactly over a short time-span $[0, (p-1)H]$ and using function values

$$f_k^{\{\sigma\}} := f^{\{\sigma\}}(y(kH)), \quad k = \{0, \dots, p-1\}, \quad \sigma \in \{1, \dots, N\}, \quad (32)$$

to approximate, via finite differences, the higher order derivatives needed in eq. (7). Readers interested in further details about the starting procedure may consult [20, 32]. The ending procedure for GLMs produces the high order approximation to $y(t_f)$ at the final time using stage values. All ADI-GLMs designed in this paper have the property that $\mathbf{c}_s = 1$, therefore, the last computed internal stage may be used as the final value in the integration with no further calculation required:

$$y_{t_f} = Y_s^{\{N\}} = h \sum_{\sigma=1}^N \sum_{j=1}^s a_{s,j}^{\{N,\sigma\}} f^{\{\sigma\}}(Y_j^{\{\sigma\}}) + \sum_{j=1}^r u_{s,j}^{\{N,\sigma\}} \xi_j^{\{\sigma\}[n-1]}. \quad (33)$$

Remark 7 (The ADI character of the methods). *The Butcher tableau for ADI-GLMs can be permuted to reflect the order of computation of stages in practice. In general, an ADI-GLM proceeds with computing internal stages:*

$$\left\{ Y_1^{\{1\}}, Y_1^{\{2\}}, \dots, Y_1^{\{N\}}, \dots, Y_s^{\{1\}}, \dots, Y_s^{\{2\}}, \dots, Y_s^{\{N\}} \right\}, \quad (34)$$

after which external stage updates are computed. Let us consider the application of the second order ADI-GLM eq. (35a) to eq. (14). We reorder the tableau according to the permutation list $\mathcal{P} = \{1, 3, 2, 4\}$ to get the permuted tableau

consistent times $t_{n-1} + \mathbf{c}h$. For a 3D problem we use the equation:

$$\frac{\partial u}{\partial t} = \frac{\partial^2 u}{\partial x^2} + \frac{\partial^2 u}{\partial y^2} + \frac{\partial^2 u}{\partial z^2} + g(x, y, z, t), \quad (36a)$$

$$\begin{aligned} g(x, y, z, t) = & e^t(1-x)x(1-y)y(1-z)z \\ & + 2e^t(1-x)x(1-y)y + 2e^t(1-x)x(1-z)z \\ & + 2e^t(1-y)y(1-z)z - 6e^t \\ & + e^t \left(\left(x + \frac{1}{3}\right)^2 + \left(y + \frac{1}{4}\right)^2 + \left(z + \frac{1}{2}\right)^2 \right), \end{aligned} \quad (36b)$$

with Dirichlet boundary conditions according to the exact solution:

$$u(x, y, z, t) = e^t(1-x)x(1-y)y(1-z)z \quad (37)$$

$$+ e^t \left(\left(x + \frac{1}{3}\right)^2 + \left(y + \frac{1}{4}\right)^2 + \left(z + \frac{1}{2}\right)^2 \right). \quad (38)$$

The spatial discretization uses second order finite differences on the unit cube domain $D := \{x, y, z \in [0, 1]\}$ with a uniform mesh with N_p points in each direction. We use the parameter N_p in our experiments to change the stiffness of directional derivatives. Note that using a uniform mesh allows us to factorize a tridiagonal 1D Jacobian matrix once and use it to efficiently to compute directional stages.

To verify the temporal order of convergence for the new methods, we integrate the problem over a time-span $t = [0, 1]$ and record the relative ℓ_2 error at final time versus number of time steps. Figures 1a to 1c, verify the theoretical order for a range of mesh sizes. We compare ADI-DIMSIMs with an ADI scheme based on a fourth order IMEX Runge–Kutta method reported in [33, Example 3]. We note the deterioration in the order as the problem becomes more stiff with decreasing mesh size in fig. 1d.

For a 2D numerical experiment the following problem is used on unit square domain $D = \{x, y \in [0, 1]\}$, with the same spatial discretization and integrated over the same time-span:

$$\frac{\partial u}{\partial t} = \frac{\partial^2 u}{\partial x^2} + \frac{\partial^2 u}{\partial y^2} + h(x, y, t), \quad (39a)$$

$$\begin{aligned} h(x, y, t) = & e^t(1-x)x(1-y)y + e^t \left(\left(x + \frac{1}{3}\right)^2 + \left(y + \frac{1}{4}\right)^2 - 4 \right) \\ & + 2e^t(1-x)x + 2e^t(1-y)y, \end{aligned} \quad (39b)$$

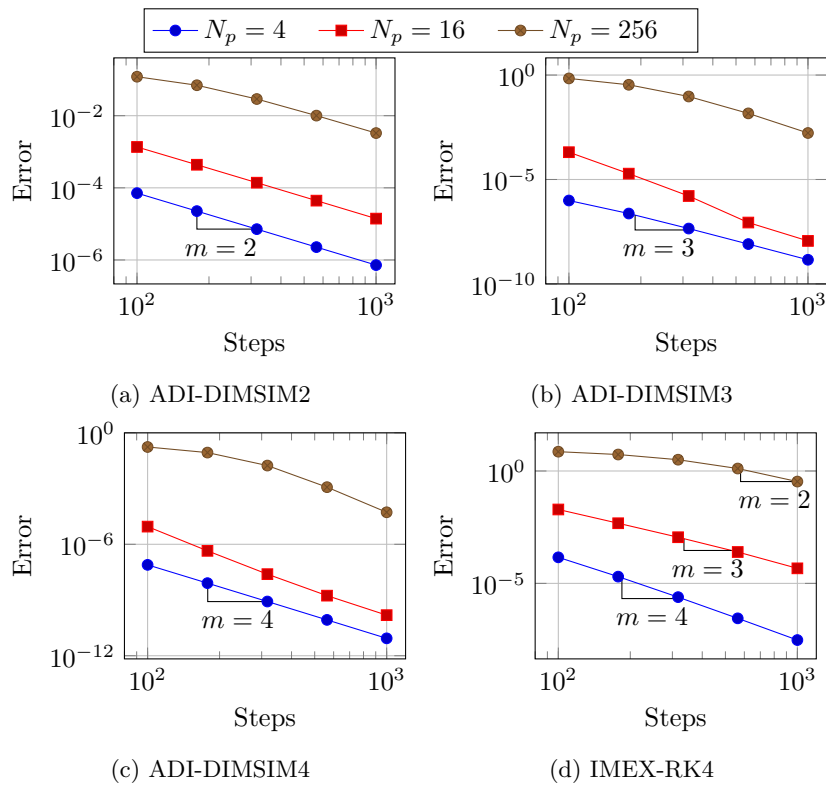


Figure 1: Convergence plots for ADI-DIMSIMs on 3D test problem compared to IMEX-RK4 method

with Dirichlet boundary conditions according to the exact solution:

$$u(x, y, t) = e^t(1-x)x(1-y)y + e^t \left(\left(x + \frac{1}{3}\right)^2 + \left(y + \frac{1}{4}\right)^2 \right). \quad (40)$$

Figure 2 shows convergence plots for this experiment. Once again, we observe

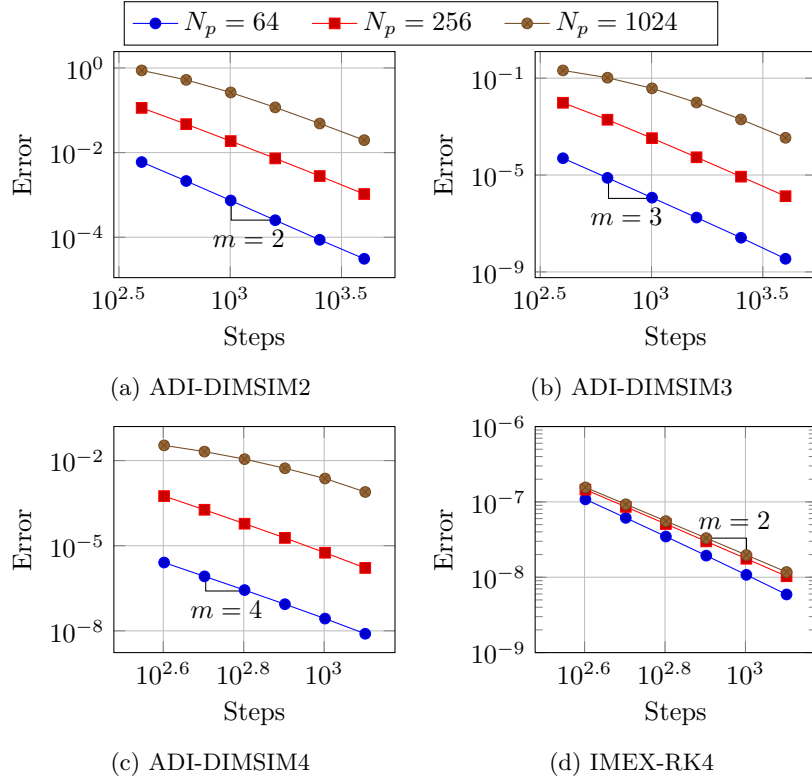


Figure 2: Convergence plots for ADI-DIMSIMs on 2D test problem compared to IMEX-RK4 method

the order reduction for the IMEX-RK4 method in fig. 2d while ADI-DIMSIMs retain their convergence order in figs. 2a to 2c.

For a third set of experiments, we examine solutions of eq. (39), this time considering the forcing term $g(x, y, t)$ as a third partition to be treated explicitly in the entire integration. This means that the Butcher tableau in eq. (13) is used for these experiments. Figure 3 summarizes the results with close to theoretical order of ADI-DIMSIMs.

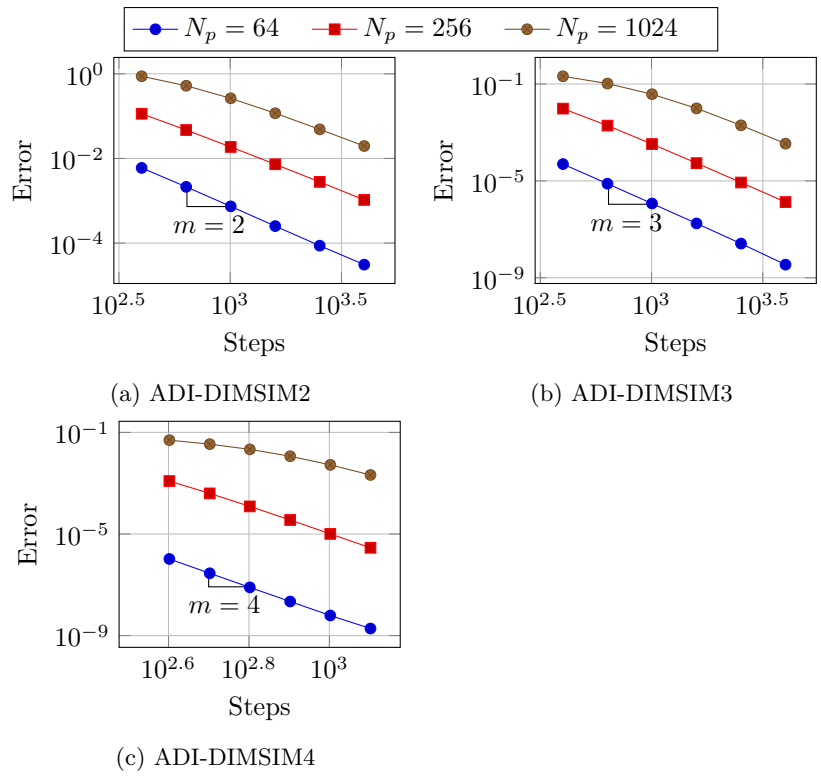


Figure 3: Convergence plots for ADI-DIMSIMs on 2D test problem with an explicit partition

8. Conclusions

This work constructs the new family of ADI-GLM schemes that perform alternating directions implicit integration in the framework of General Linear Methods. Each stage of a ADI-GLM scheme is implicit in a single component of the method, and is explicitly coupled to the other components. This ensures a high computational efficiency. The ADI character of the method stems from the fact that consecutive stages are implicit in different partitions, thereby “alternating directions.” Order conditions and stability of these methods are investigated theoretically. The ADI-GLM structure allows for high stage order approximations, and this property alleviates the order reduction observed with other families of schemes.

Using the new ADI-GLM theory we construct practical ADI-DIMSIMS of orders two, three, and four. Their design emphasizes stability when applied to parabolic systems where each component has a Jacobian with real negative eigenvalues. The stability analysis and plots show the new schemes are well-suited for these problems. Numerical experiments show that the new methods retain their high order of accuracy when applied to parabolic equations with time-dependent Dirichlet boundary conditions where other ADI methods suffer from order reduction.

The future directions for the authors include extending the current set of methodology to design methods suited for hyperbolic and oscillatory systems and numerical experiments highlighting the computational efficiency of ADI-DIMSIMS on large scale problems.

Acknowledgments

This work was funded by awards NSF CCF-1613905, NSF ACI-1709727, AFOSR DDDAS FA9550-17-1-0015, and by the Computational Science Laboratory at Virginia Tech. The authors would like to thank Prof. Domingo Hernández Abreu for his valuable comments on this manuscript.

References

References

- [1] J. Douglas, On the numerical integration of $u_{x,x} + u_{y,y} = u_t$ by implicit methods, *SIAM* 3 (1955) 42–65.
- [2] J. Douglas, H. H. Rachford, On the numerical solution of heat conduction problems in two and three space variables, *Transactions of the American Mathematical Society* 82 (1956) 421–439.
- [3] D. Peaceman, H. Rachford, The numerical solution of parabolic and elliptic differential equations, *Journal of Society for Industrial and Applied Mathematics* 3 (1955) 28–42.

- [4] G. Strang, On the construction and comparison of difference schemes, *SIAM Journal on Numerical Analysis* 5 (1968) 506–517.
- [5] H. Yoshida, Construction of higher order symplectic integrators, *Physics Letters* 150 (1990) 262–268.
- [6] N. Yanenko, *The Method of Fractional-Steps*, Springer, Berlin Heidelberg NewYork, 1971.
- [7] S. González-Pinto, D. Hernández-Abreu, S. Pérez-Rodríguez, Rosenbrock-type methods with inexact AMF for the time integration of advection–diffusion–reaction PDEs, *Journal of Computational and Applied Mathematics* 262 (2014) 304–321. doi:10.1016/j.cam.2013.10.050.
- [8] S. González-Pinto, D. Hernández-Abreu, S. Pérez-Rodríguez, AMF–Runge–Kutta formulas and error estimates for the time integration of advection diffusion reaction PDEs, *Journal of Computational and Applied Mathematics* 289 (2015) 3–21. doi:10.1016/j.cam.2015.03.048.
- [9] S. González-Pinto, E. Hairer, D. Hernández-Abreu, S. Pérez-Rodríguez, AMF–type W–methods for parabolic problems with mixed derivatives, *SIAM Journal on Scientific Computing* 40 (5) (2018) A2905–A2929. doi:10.1137/17M1163050.
- [10] H. Zhang, A. Sandu, P. Tranquilli, Application of approximate matrix factorization to high-order linearly-implicit Runge-Kutta methods, *Journal of Computational and Applied Mathematics* 286 (2015) 196–210. doi:10.1016/j.cam.2015.03.005.
- [11] B. Bujanda, J. Jorge, Stability results for fractional-step discretizations of time dependent coefficient evolutionary problems, *Applied Numerical Mathematics* 38 (2001) 69–86.
- [12] B. Bujanda, J. Jorge, Fractional-step Runge–Kutta methods for time dependent coefficient parabolic problems, *Applied Numerical Mathematics* 45 (2003) 99–122.
- [13] A. Prothero, A. Robinson, On the stability and accuracy of one-step methods for solving stiff systems of ordinary differential equations, *Mathematics of Computation* 28 (125) (1974) 145–162.
- [14] A. Ostermann, M. Roche, Runge–Kutta methods for partial differential equations and fractional orders of convergence, *Mathematics of computation* 59 (200) (1992) 403–420.
- [15] M. Braś, A. Cardone, Z. Jackiewicz, B. Welfert, Order reduction phenomenon for general linear methods, *Applied Numerical Mathematics* 119 (2017) 94 – 114. doi:10.1016/j.apnum.2017.04.001.

- [16] L. Portero, J. Jorge, B. Bujanda, Avoiding order reduction of fractional step Runge–Kutta discretizations for linear time dependent coefficient parabolic problems, *Applied Numerical Mathematics* 48 (3) (2004) 409 – 424. doi:10.1016/j.apnum.2003.11.006.
- [17] Z. Jackiewicz, *General Linear Methods for Ordinary Differential Equations*, Wiley, Hoboken, New Jersey, 2009.
- [18] J. Butcher, General linear methods for stiff differential equations, *BIT* 41 (2) (2001) 240–264. doi:10.1023/A:1021986222073.
- [19] J. Butcher, W. Wright, The construction of practical general linear methods, *BIT* 43 (4) (2003) 695–721. doi:10.1023/B:BITN.0000009952.71388.23.
- [20] H. Zhang, A. Sandu, S. Blaise, Partitioned and implicit-explicit general linear methods for ordinary differential equations, *Journal of Scientific Computing* 61 (1) (2014) 119–144. doi:10.1007/s10915-014-9819-z.
- [21] H. Zhang, A. Sandu, A second-order diagonally-implicit-explicit multi-stage integration method, in: *Proceedings of the International Conference on Computational Science ICCS 2012*, Vol. 9, 2012, pp. 1039–1046. doi:10.1016/j.procs.2012.04.112.
- [22] A. Cardone, Z. Jackiewicz, A. Sandu, H. Zhang, Construction of highly stable implicit-explicit general linear methods, in: *AIMS proceedings*, Vol. *Dynamical Systems, Differential Equations, and Applications*, Madrid, Spain, 2015. doi:10.3934/proc.2015.0185.
- [23] H. Zhang, A. Sandu, S. Blaise, High order implicit–explicit general linear methods with optimized stability regions, *SIAM Journal on Scientific Computing* 38 (3) (2016) A1430–A1453. doi:10.1137/15M1018897.
- [24] E. Zharovsky, A. Sandu, H. Zhang, A class of IMEX two-step Runge-Kutta methods, *SIAM Journal on Numerical Analysis* 53 (1) (2015) 321–341. doi:10.1137/130937883.
- [25] G. Izzo, Z. Jackiewicz, Transformed implicit-explicit DIMSIMs with strong stability preserving explicit part, *Numerical Algorithms* 81 (4) (2019) 1343–1359. doi:10.1007/s11075-018-0647-3.
- [26] M. Schneider, J. Lang, W. Hundsdorfer, Extrapolation–based super-convergent implicit–explicit Peer methods with A–stable implicit part, *Journal of Computational Physics* 367 (2018) 121 – 133. doi:10.1016/j.jcp.2018.04.006.
- [27] M. Schneider, J. Lang, R. Weiner, Super-convergent implicit-explicit peer methods with variable step sizes, *arXiv preprint arXiv:1902.01161*.

- [28] H. Zhang, A. Sandu, S. Blaise, High order implicit-explicit general linear methods with optimized stability regions, *SIAM Journal on Scientific Computing* 38 (3) (2016) A1430–A1453.
- [29] J. Butcher, Z. Jackiewicz, Diagonally implicit general linear methods for ordinary differential equations, *BIT* 33 (3) (1993) 452–472. doi:10.1007/BF01990528.
- [30] Z. Jackiewicz, *General linear methods for ordinary differential equations*, John Wiley & Sons, 2009.
- [31] J. Butcher, Z. Jackiewicz, Diagonally implicit general linear methods for ordinary differential equations, *BIT Numerical Mathematics* 33 (3) (1993) 452–472.
- [32] G. Califano, G. Izzo, Z. Jackiewicz, Starting procedures for general linear methods, *Applied Numerical Mathematics* 120 (2017) 165–175.
- [33] A. Sandu, M. Günther, A generalized-structure approach to additive Runge-Kutta methods, *SIAM Journal on Numerical Analysis* 53 (1) (2015) 17–42. doi:10.1137/130943224.
- [34] A. Sarshar, S. Roberts, A. Sandu, ADI-GLM coefficients, *Mendeley Data* (2019). doi:10.17632/cxnhv3m2sx.2.
- [35] J. Butcher, Diagonally-implicit multi-stage integration methods, *Applied Numerical Mathematics* 11 (5) (1993) 347–363. doi:10.1016/0168-9274(93)90059-Z.
- [36] J. Butcher, Z. Jackiewicz, Construction of diagonally implicit general linear methods of type 1 and 2 for ordinary differential equations, *Applied Numerical Mathematics* 21 (4) (1996) 385–415. doi:10.1016/S0168-9274(96)00043-8.

Appendix A. ADI-GLMs

This section includes the newly developed ADI-DIMSIMS of orders two, three, and four. MATLAB files containing these coefficients are also available in [dataset] [34].

Appendix A.1. ADI-DIMSIM2

We use an L-stable implicit base method from [35] for ADI-DIMSIM2.

$$\begin{aligned}
\mathbf{A}^{\{I\}} &= \begin{bmatrix} \frac{2-\sqrt{2}}{2} & 0 \\ \frac{2(\sqrt{2}+3)}{7} & \frac{2-\sqrt{2}}{2} \end{bmatrix}, & \mathbf{B}^{\{I\}} &= \begin{bmatrix} \frac{73-34\sqrt{2}}{28} & \frac{4\sqrt{2}-5}{4} \\ \frac{3(29-16\sqrt{2})}{28} & \frac{34\sqrt{2}-45}{28} \end{bmatrix}, \\
\mathbf{W}^{\{I\}} &= \begin{bmatrix} 1 & \frac{\sqrt{2}-2}{2} & 0 \\ 1 & \frac{3(\sqrt{2}-4)}{14} & \frac{\sqrt{2}-1}{2} \end{bmatrix}, & \mathbf{A}^{\{E\}} &= \begin{bmatrix} 0 & 0 \\ \frac{3}{2} & 0 \end{bmatrix}, \\
\mathbf{B}^{\{E\}} &= \begin{bmatrix} \frac{1}{\sqrt{2}} & \frac{3-\sqrt{2}}{4} \\ \frac{\sqrt{2}-1}{2} & \frac{3-\sqrt{2}}{4} \end{bmatrix}, & \mathbf{W}^{\{E\}} &= \begin{bmatrix} 1 & 0 & 0 \\ 1 & -\frac{1}{2} & \frac{1}{2} \end{bmatrix}, \\
v &= \begin{bmatrix} \frac{3-\sqrt{2}}{2} & \frac{\sqrt{2}-1}{2} \end{bmatrix}^T, & \mathbf{c} &= \begin{bmatrix} 0 & 1 \end{bmatrix}^T.
\end{aligned}$$

Appendix A.2. ADI-DIMSIM3

We use an L-stable implicit base method from [36] for ADI-DIMSIM3. The following coefficients are rational approximations to the exact coefficients accurate to 24 digits.

$$\begin{aligned}
\mathbf{A}^{\{I\}} &= \begin{bmatrix} \frac{129981159316}{298213221025} & 0 & 0 \\ \frac{472981046840}{1888035733227} & \frac{129981159316}{298213221025} & 0 \\ -\frac{408860438935}{337456558734} & \frac{1049716501919}{1048380236594} & \frac{129981159316}{298213221025} \end{bmatrix}, \\
\mathbf{B}^{\{I\}} &= \begin{bmatrix} \frac{818629988268}{981817092145} & \frac{735879558291}{1139134361459} & -\frac{96693387431}{306159262034} \\ \frac{435713380671}{718693545019} & \frac{3397277300866}{2639826970205} & -\frac{581689679739}{1212506039656} \\ -\frac{164008995335}{531777165056} & \frac{3204278525979}{842472621931} & -\frac{1170634530631}{1044535547981} \end{bmatrix}, \\
\mathbf{W}^{\{I\}} &= \begin{bmatrix} 1 & -\frac{129981159316}{298213221025} & 0 & 0 \\ 1 & -\frac{63231801579}{339260252164} & -\frac{94226735668}{1013918320559} & -\frac{50172116077}{1490999795865} \\ 1 & \frac{1224205243956}{1580735023225} & -\frac{377260820095}{864278390147} & -\frac{145496067686}{824686465859} \end{bmatrix}, \\
\mathbf{A}^{\{E\}} &= \begin{bmatrix} 0 & 0 & 0 \\ \frac{692830401049}{1119419041371} & 0 & 0 \\ -\frac{974910195245}{1036334372568} & \frac{1458124485343}{1218848111125} & 0 \end{bmatrix}, \\
\mathbf{B}^{\{E\}} &= \begin{bmatrix} \frac{274198327012}{348784765929} & \frac{335124252337}{1242427076379} & \frac{256046237035}{1044616400532} \\ \frac{2367946890051}{2381074405894} & -\frac{395462379375}{996294720374} & \frac{391448928279}{669688356392} \\ \frac{1211513153203}{1601457627995} & \frac{473388990672}{901108379101} & \frac{1335987676745}{1749669440649} \end{bmatrix}, \\
\mathbf{W}^{\{E\}} &= \begin{bmatrix} 1 & 0 & 0 & 0 \\ 1 & -\frac{105007291910}{883010702197} & \frac{1}{8} & \frac{1}{48} \\ 1 & \frac{6500435948486}{8732264247243} & -\frac{119638187109}{1218848111125} & \frac{25266119777}{1475180609484} \end{bmatrix}, \\
v &= \begin{bmatrix} \frac{1611220452657}{2918396719813} & \frac{626900045900}{853091602939} & -\frac{165394139815}{576391394057} \end{bmatrix}^T, \\
\mathbf{c} &= \begin{bmatrix} 0 & \frac{1}{2} & 1 \end{bmatrix}^T.
\end{aligned}$$

Appendix A.3. ADI-DIMSIM4

Appendix B. Stability of ADI-GLMs

$$\begin{aligned}
\mathbf{A}\{I\} &= \begin{bmatrix} \frac{2}{5} & 0 & 0 & 0 \\ \frac{1}{155} & \frac{2}{5} & 0 & 0 \\ -\frac{3}{127} & \frac{31}{72} & \frac{2}{5} & 0 \\ \frac{6}{139} & \frac{12}{19} & \frac{29}{95} & \frac{2}{5} \end{bmatrix}, & \mathbf{B}\{I\} &= \begin{bmatrix} \frac{25640275033859}{233564187988800} & \frac{405169687}{540615360} & \frac{1089772729}{8109230400} & \frac{70445177}{426801600} \\ \frac{89870426730779}{233564187988800} & \frac{545995987}{1621846080} & \frac{13906861889}{8109230400} & \frac{1223893451}{4410283200} \\ \frac{292292722987739}{233564187988800} & \frac{5722388059}{1621846080} & \frac{5251926081}{901025600} & \frac{115646334041}{54203803200} \\ \frac{12591629268162881}{4437719571787200} & \frac{4936252337}{540615360} & \frac{102615203329}{8109230400} & \frac{5841129112303}{1127183025600} \end{bmatrix}, \\
\mathbf{W}\{I\} &= \begin{bmatrix} 1 & -\frac{2}{5} & 0 & 0 \\ 1 & \frac{34}{465} & -\frac{7}{90} & -\frac{13}{810} \\ 1 & -\frac{6413}{45720} & -\frac{203}{1080} & -\frac{137}{2160} \\ 1 & -\frac{5018}{13205} & -\frac{179}{570} & -\frac{233}{1710} \end{bmatrix}, & \mathbf{A}\{E\} &= \begin{bmatrix} 0 & 0 & 0 & 0 \\ \frac{768}{7129} & 0 & 0 & 0 \\ \frac{2699}{8714} & \frac{4969}{11444} & 0 & 0 \\ \frac{2629}{3049} & \frac{2643}{20780} & \frac{11707}{22938} & 0 \end{bmatrix}, \\
\mathbf{B}\{E\} &= \begin{bmatrix} \frac{9887514441977875393}{8084061960608111040} & \frac{75125403707867}{1268701473326400} & \frac{200041286909}{326332503360} & \frac{5924747}{85360320} \\ \frac{887006696901861513}{8084061960608111040} & \frac{727096994167267}{1268701473326400} & \frac{67370070011}{326332503360} & \frac{119019300359}{202844573760} \\ \frac{17771936994130966829533}{23128501269299805685440} & \frac{249067742877763}{140966830369600} & \frac{519937182674317}{311212430704320} & \frac{940676971064501}{1064048569640640} \\ \frac{8566493244911672759404729}{32110678261545596037650880} & \frac{17071987325364576461}{4850245732526827200} & \frac{257098496412689}{67811894198208} & \frac{275159340062707361}{206758465410336192} \end{bmatrix}, \\
\mathbf{W}\{E\} &= \begin{bmatrix} 1 & 0 & 0 & 0 \\ 1 & \frac{4825}{21387} & \frac{1}{18} & \frac{1}{1944} \\ 1 & -\frac{11557817}{149584524} & \frac{7981}{102996} & \frac{30869}{5561784} \\ 1 & -\frac{363193513153}{726655425180} & \frac{83904703}{714977460} & \frac{302650439}{19304391420} \end{bmatrix}, \\
v &= \begin{bmatrix} \frac{3}{40} & -\frac{77}{277} & -\frac{41}{107} & \frac{1880483}{1185560} \end{bmatrix}^T, & \mathbf{c} &= \begin{bmatrix} 0 & \frac{1}{3} & \frac{2}{3} & 1 \end{bmatrix}^T.
\end{aligned}$$

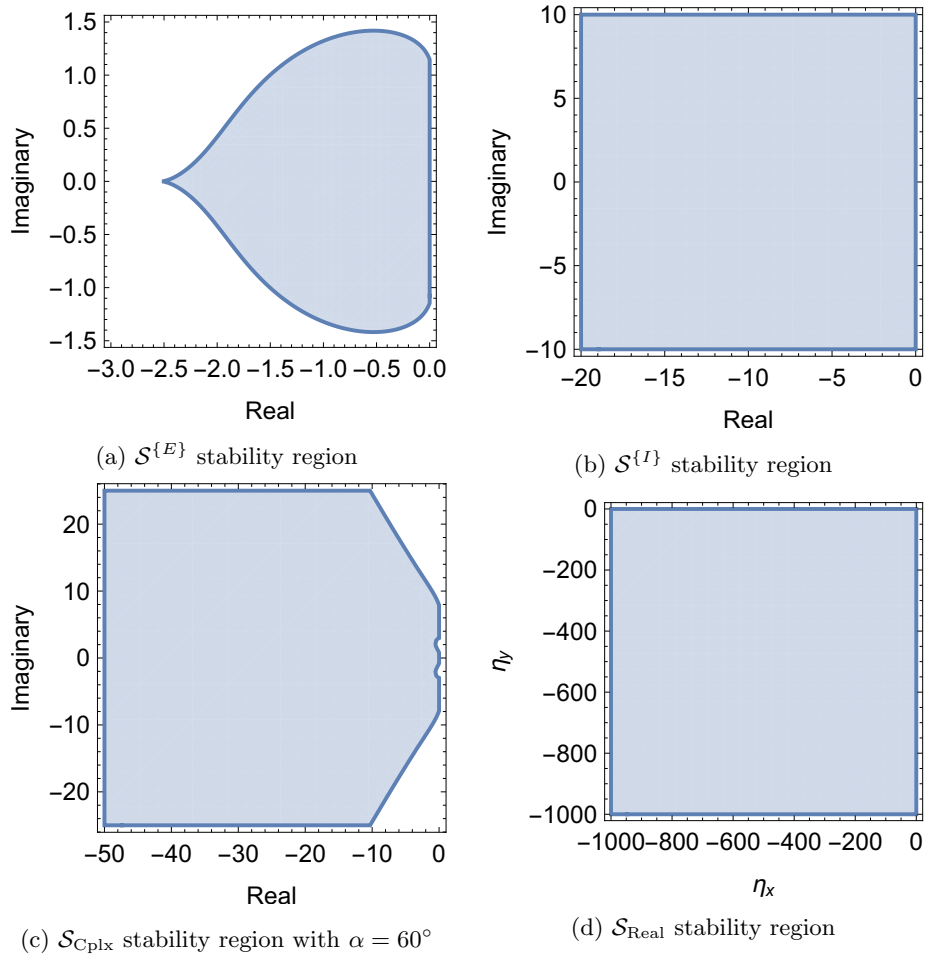


Figure B.4: Stability plots for ADI-DIMSIM2

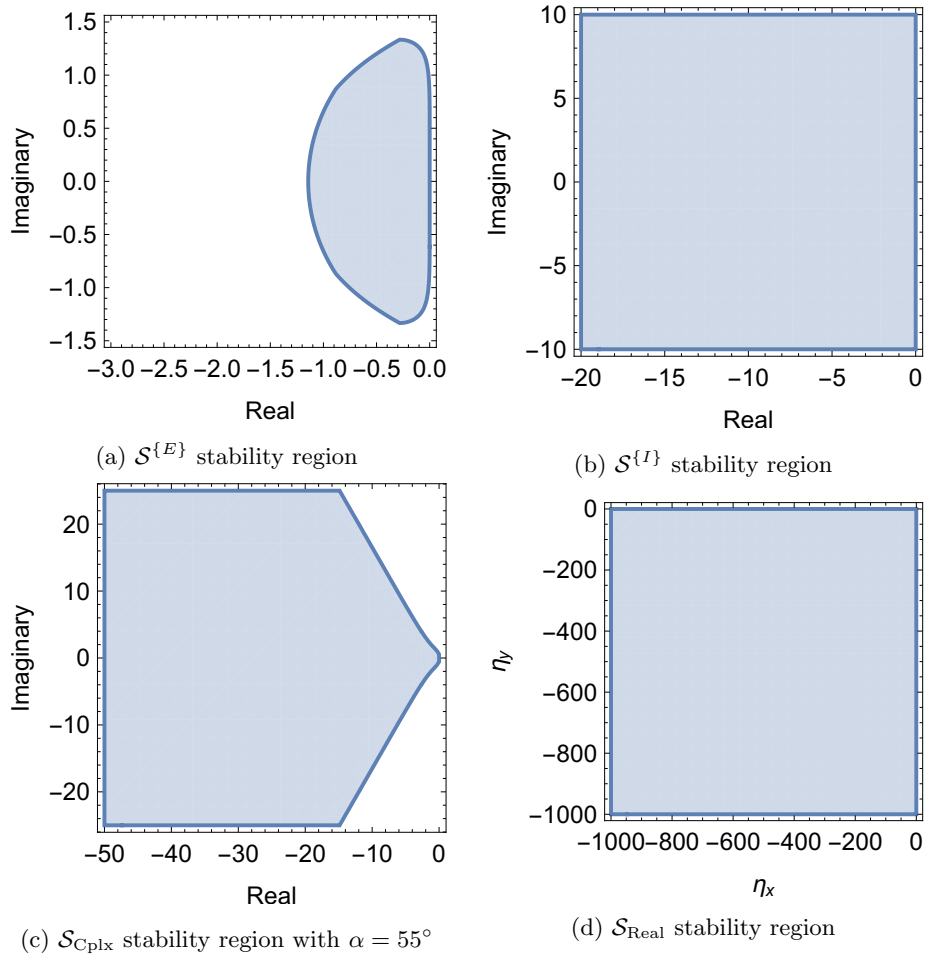


Figure B.5: Stability plots for ADI-DIMSIM3

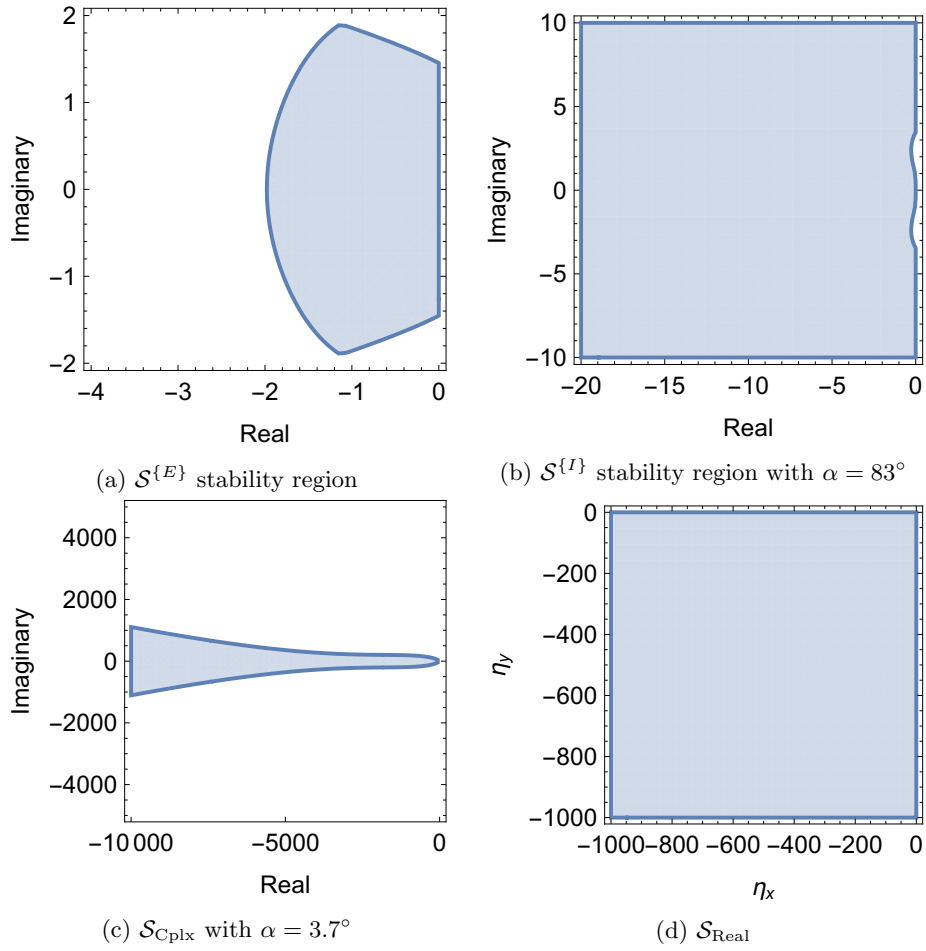


Figure B.6: Stability plots for ADI-DIMSIM4